# Orientation Dynamics and Correlations in Hairy-Rod Polymers: Concentrated Regime

**G. Petekidis, D. Vlassopoulos, and G. Fytas***

*Foundation for Research and Technology−Hellas, Institute of Electronic Structure and Laser, P.O. Box 1527, 711 10 Heraklion, Crete, Greece*

**R. Rülkens and G. Wegner**

*Max-Planck Institut für Polymerforschung, P.O. Box 3148, 55021 Mainz, Germany*

*Received March 23, 1998; Revised Manuscript Received June 29, 1998*

ABSTRACT: We report on the dynamics of orientation fluctuations in substituted poly(*p*-phenylenes) using dynamic depolarized light scattering. These model hairy-rod polymers, with large inherent optical anisotropy, exhibit enhanced solubility and allow investigation of their dynamics in molecularly dispersed isotropic solutions and concentrations as high as 60 wt %. The high-quality intermediate scattering functions reveal a bimodal relaxation for the orientation fluctuations. Whereas the fast process has an intensity decreasing with the scattering wavevector $q$ following a Debye-like behavior and a rotational relaxation rate with an intercept, the features of the slow mode, exhibiting a broad distribution of relaxation times, are surprisingly opposite: the intensity increases and the rate decreases with $q$. The concentration dependence of these relaxation modes at different solvents support the notion of unchanged chain conformation and interactions and indicate a slowing down, which is more pronounced for the slow relaxation. With the additional support of dynamic shear rheological measurements, which provide information on the overall rotational motion of these semistiff chains, we attribute the fast process to the collective rotational motion of the Kuhn segments of the persistent poly(*p*-phenylene) chains and the slow one to the cooperative motion of orientationally correlated pairs of segments.

## I. Introduction

The pertinent features of rigid-rod polymers, which relate to their technological and scientific importance, are associated with their highly anisotropic shape, the formation of mesophases, their anisotropic diffusion, and the translation−rotation coupling. There is already a significant amount of theoretical and experimental work accumulated on these topics.[1−3] However, the dynamic behavior of stiff-chain molecules, affected by the above features, still remains virtually unexplored and represents a great scientific challenge. Rodlike polymers offer the potential for a detailed study of the reorientational dynamics, due to their anisotropic molecular shape; the main reason these polymers have not received much attention is the lack of well-characterized optically anisotropic model systems.

Investigations of the orientational dynamics have mostly concentrated on stiff poly($\gamma$-benzyl α-L-glutamate), which is known to form nematic mesophases at high concentrations; they were carried out mostly by electric birefringence,[1] whereas dynamic light scattering experiments, due to the small optical anisotropy of these systems, resulted in difficult and sometimes ambiguous measurements.[4] Recent advances in macromolecular chemistry have led to the synthesis of well-defined poly(*p*-phenylenes), PPP, with solely aliphatic $C_{12}$ side chains, with varying molecular weights and much higher optical anisotropy compared to other macromolecules.[5] On the other hand, their persistent length is relatively low when compared to polymeric liquid crystals, such as poly($\gamma$-benzyl L-glutamate).[6] This means that PPPs cannot be considered as true rigid rods, but rather wormlike chains, as discussed throughout this work (see also ref 6). Well-resolved measurements of orientational dynamics with these polymers were carried out with photon correlation spectroscopy (PCS)[7] in semidilute solutions, yielding two relaxation modes.[8,9] These measurements, however, presented two complications: First, and most importantly, PPP exhibits a dissolution problem as the concentration increases; it is due to clustering, despite the presence of side chains, whose role is solely to increase solubility. Thus, it is not clear to what extend these results reflect truly molecular properties and how the dynamics and kinetics of aggregation influence them. Second, it is evident from these studies, that a complete understanding of the dynamics requires a systematic study of both concentration and orientation relaxation functions.

From the above, it is evident that there is a clear need for well-defined experiments with model systems, to resolve the present ambiguities and confusion related to the dynamics of rodlike polymers, e.g., the control of the aggregation process and the resolution of the various relaxation mechanisms. This will elucidate the effects of concentration and provide the necessary ingredients for the assessment of the theoretical predictions. To address this challenge, it is necessary to detect truly molecular relaxation processes. Our recent efforts with PPPs yielded a means to control the growth of clusters in such highly anisotropic semiflexible polymers,[9] but investigations in various solvents clearly restricted the measurements of reorientational dynamics to rather low concentrations in the semidilute regime. Even in this concentration range, the presence of aggregates was detected, and their effects on the dynamics were evident.[8,9] The main result of our studies in the depolarized (VH) scattering geometry was the observation of a relaxation mechanism that increased in both intensity and characteristic time with the scattering wavevector, $q$; this process was attributed to orientational correla-

S0024-9297(98)00450-1 CCC: $15.00 
Published on Web 08/19/1998

tions in space due to some kind of local ordering of parts of the molecules. However, the restrictions in the upper limit of the concentrations (typically 6 wt %) inhibited a further elucidation of the characteristics and molecular origin of these phenomena.

The availability of hairy-rod poly(*p*-phenylenes), substituted by bulky aromatic sulfonate esters, helped in overcoming this important difficulty.[10] These macromolecules are soluble at very high concentrations (typically 60 wt %), while in the isotropic regime, and this allows a systematic investigation of their orientational dynamics, extending the previous work and eliminating any complications from aggregation. This represents the scope of the research discussed below. It is noted that the dynamic structure of these polymers in solution (concentration fluctuations) is discussed in a subsequent paper.[11] Section II of this paper reviews the relevant theories on the reorientational dynamics of rodlike and semiflexible polymers in isotropic solutions, as well as the basics of dynamic depolarized light scattering. Section III describes the materials and experimental methods used, whereas the main findings are presented in section IV.A. A thorough discussion of the pertinent experimental findings is presented in sections IV.B−D, while the conclusions from this work are summarized in section V.

## II. Theoretical Background

**A. Rotational Dynamics.** For dilute rigid rods the rotational diffusion coefficient assumes the form[2,12]

$$D_{R0} = (3k_B T/\pi\eta_s L^3)\,[\ln(2L/b) - \zeta] \qquad (1)$$

with $\eta_s$ being the solvent viscosity, $L$ the length and $b$ the diameter of the rod, and $\zeta$ a function of the aspect ratio ($L/b$), which describes the corrections due to end effects. The rotational dynamics in the semidilute and the concentrated regions are largely affected by intermolecular interactions, in contrast to the dilute region where they are negligible. The concentration dependence of the diffusion coefficients for solutions of rodlike and semistiff macromolecules is still under investigation although there are many studies.[1−3,12]

The first theory for the dynamics of concentrated solutions of rigid rods was presented by Doi and Edwards (DE).[12] In its simplest form, DE theory is a scaling theory based on the reptation concept that was used earlier for flexible chains. It was formulated for infinitely thin, uncharged, rigid rods whose only interaction is that they cannot pass through each other. Thus, the solution is thermodynamically ideal but, because there are strong effects of hard-line intermolecular interactions on the molecular kinetics, the system is kinetically nonideal. DE proposed that the substantial restrictions on the rods motions can be modeled by using the concept of an effective tube of radius $\alpha$ which is formed by the neighboring rods; from geometrical considerations, $\alpha = 2/(\pi\rho L^2)$, with $\rho$ being the number concentration. Inside this tube the rodlike molecules can move freely along the axes of the tube, while the translation in the perpendicular direction is restricted to about a distance $\alpha$ due to the presence of the neighboring rods. The effect of the mutual hindrance on the rod's rotation is much more drastic than that on the translational diffusion. The former involves a rotation within the time $\tau_d \approx L^2/D_{||,0} \approx 1/D_{R,0}$ necessary for the rod to diffuse along its initial tube and escape from it. Hence, in this reptation mechanism, the rotational diffusion $D_R \approx (\alpha/L)^2/\tau_d$ reads[12]

$$D_R = \beta D_{R,0}(\rho L^3)^{-2} \qquad (2)$$

where $\beta^{1/2}$ represents a maximum crowding of rods. In the original DE theory $\beta$ was expected to assume values between 1 and 10. It is observed, however, that $\beta$ is rather of the order of $10^3$ suggesting that the caging effects start at much higher concentration than was initially thought.[13]

Experimental results and theoretical considerations led to the need for modifications of the original DE theory, i.e., a recalculation of the tube size and geometry, different cage escape mechanisms, finite thickness of the rod molecules, and chain flexibility effects.[1,13,14] The latter, being the common case for real rigid chains, can have important effects on the dynamic behavior, and very often deviations between experiments and theory of rods are attributed to it. For instance, a flexible end of a stiff macromolecule has some freedom to choose its own path when translating along its length, despite the fact that a large part of the chain may be caged and thus restricted to a certain orientation. The wormlike model has been in many cases the basis of the theoretical approaches describing the dynamics of semistiff chains in the dilute regime as well as at high concentrations. Another model for investigating the dynamics of semiflexible molecules is the fuzzy cylinder model.[3,15]

For a wormlike chain, the effect of flexibility is large when the mean square deflection of the chain from linearity is larger than the average cage size $\alpha$, i.e., at high concentrations. Since segments of one persistence length ($l$) long can be considered to rotate in a statistically independent manner, the account of the cage size effect around a segment leads to a concentration-independent rotational diffusion coefficient. However, over the contour length range $\alpha < L < \alpha^{2/3}\, l^{1/3}$, the rotational diffusion coefficient is determined by the reptation-rotation of the rod and depends on concentration through the change of the cage size $\alpha$ with concentration.[16] Same conclusions hold for the description of the Brownian dynamics of semiflexible polymers in concentrated solutions assuming only reptational motion of the chain and were reached by Doi.[17] In a scaling approach, Semenov investigated the dynamics of concentrated solutions of stiff polymers in isotropic solutions.[18] The orientation relaxation function of the persistent chain with $L \gg l$ in the concentrated regime is nonexponential and its long time decay is given by the concentration independent characteristic time $\tau_R \approx L^2/D \propto L^3$, i.e., the same scaling behavior with linear entangled flexible chain.

In the "fuzzy cylinder" model, the global motion of the semiflexible chain can be identified with that of a segment-distribution model with a cylindrical symmetry.[3,15] The cylinder has a length equal to the root-mean-square end-to-end distance of the wormlike chain, $L_e = \langle R^2\rangle^{1/2}$, and an effective diameter, $b_e = [\langle H(L/2)^2\rangle + b^2]^{1/2}$, with $\langle H(L/2)^2\rangle$ the mean square distance of the chain midpoint from the end-to-end displacement axis and $b$ the diameter of the chain. In contrast to the previous considerations of semiflexible chains, this model allows internal motion of the stiff chain. Under these conditions, the rotational diffusion coefficient is predicted to exhibit a weaker than $c^{-2}$ dependence in the intermediate concentrations, whereas at high con-

centrations it can decrease further due to the decrease of $D_{||}$.

**B. Dynamic Depolarized Light Scattering.** The dynamics of collective orientation fluctuations in a dense polymer system can, in principle, be obtained from the depolarized Rayleigh spectrum measured in the so-called VH scattering geometry; incident beam and scattered light are polarized vertically and horizontally to the scattering plane, respectively. Within the Rayleigh−Debye approximation, the time correlation function of the scattered field with wave vector $q$ contains the summations over pairs of segments of the same and different polymer chains[6,19]

$$I_{VH}(q,t) = \langle \sum_{P,Q}^{N} \sum_{l,m}^{n} \alpha_P{}^l(0)\, \alpha_Q{}^m(t) \exp\, iq\,(r_Q{}^m(t) - r_P{}^l(0)) \rangle \tag{3}$$

where the indices $P$ and $Q$ refer to the $N$ different chains in the scattering volume, the indices $l$ and $m$ refer to the $n$ segments associated with each polymer chain, $r_Q{}^m$ denotes the position of the $m$ th segment on the $Q$th chain, and $\alpha_Q{}^m(t)$ is the anisotropic component of the optical polarizability of the $m$ th segment. For noninteracting polymer chains, e.g., where only the self-part ($P = Q$), of the correlation function survives, eq 3 simplifies to

$$I_{VH}(q,t) = N \langle \sum_{l,m}^{n} \alpha^1(0)\, \alpha'''(t) \exp\, iq\,(r_1(t) - r_m(0)) \rangle \tag{4}$$

where the indices $l$ and $m$ run over segments of the same chain.

For a dilute solution of short ($qL < 1$) chains consisting of $n$ identical cylindrically symmetric segments and statistically independent translational and rotational motion, $I_{VH}(q,t)$ (eq 4) is a single-exponential decay function

$$I_{VH}(q,t) = \frac{N^2}{15}\langle \gamma^2 \rangle \exp[-(6D_R + Dq^2)t] \tag{5}$$

where $\langle \gamma^2 \rangle$ is the mean square of the molecular optical anisotropy and $D$ and $D_R$ are the translational and rotational diffusion of the optically anisotropic chain, respectively. According to eq 5, at $q = 0$ the depolarized correlation function depends only on the rotation of the molecule, since the translational contribution to the rate, $\Gamma_{VH}$ ($=q^2D + 6D_R$) is eliminated and the intensity $I_{VH}$ ($=N\beta^2/15$) is $q$-independent.

At finite concentrations, there is always some interference of the scattered light from different chains. When the intermolecular interactions do not vanish, the pair term in eq 3 must be kept. For concentrated solutions of rigid rods, the time correlation function of eq 3 was calculated in the framework of random phase approximation and with the help of the fluctuation−dissipation theorem.[20,21] The general form of the time correlation function of the scattered field as given by Maeda[21] is

$$I(\mathbf{q},t) = \frac{L}{4\pi}\int_t^\infty dt' \int d\mathbf{u} E(\mathbf{q},\mathbf{u}) \exp[-t'\Gamma(\mathbf{q})]\Theta(\mathbf{q})E^*(\mathbf{q},\mathbf{u}) \tag{6}$$

where $\mathbf{u}$ is the orientation of the rod, $s(\mathbf{q},\mathbf{u}) = (1/L)\int_{-L/2}^{L/2} \exp(i\mathbf{q}\cdot\mathbf{u}s)\, ds$ expresses the intramolecular interference, $E(\mathbf{q},\mathbf{u}) = \alpha(\mathbf{u})s(\mathbf{q},\mathbf{u})$, and the rate $\Gamma(\mathbf{q}) = \Theta(\mathbf{q})\cdot\Phi(\mathbf{q})$, where $\Theta(\mathbf{q})$ and $\Phi(\mathbf{q})$ are the operators for the translational−rotational diffusion of the rod and the rod−rod interactions in the mean field approximation, respectively. In Maeda's approach for the calculation of $I(\mathbf{q},t)$ of rods, one gets[21]

$$\Phi(\mathbf{q})E(u) = \int d\mathbf{u}'\left[\delta(\mathbf{u} - \mathbf{u}') + \frac{\rho}{4\pi}w(\mathbf{q}, \mathbf{u}, \mathbf{u}')\right]E(u') \tag{7}$$

with $w(\mathbf{q},\mathbf{u},\mathbf{u}')$ the spatial Fourier transform of a hard rod short-range interaction potential $w(\mathbf{r},\mathbf{u},\mathbf{u}') = w(\mathbf{u},\mathbf{u}')\delta(\mathbf{r})$ between two rods in the configurations $(\mathbf{r},\mathbf{u})$ and $(\mathbf{r}',\mathbf{u}')$. If the radial part of the potential involves long-range interactions, $\delta(\mathbf{r})$ will be substituted by a more realistic function introducing a correlation length $\xi$. The orientation distribution of rods affects $I(q,t)$ through $E(\mathbf{q},\mathbf{u})$. For random orientational fluctuation correlations persisting up to some coherence distance $\xi$, the intensity $I(q)$ is $q$-dependent and peaks at $q = 0$. The functional form of $I(q)$ depends on the decay of the orientation correlation function $f(r) = 3\langle \mathbf{u}_i\mathbf{u}_j \rangle - 1$ in real space, affecting the interaction $\Phi(\mathbf{q})$. In general, $I(q,t)$ from eq 6 exhibits a nonexponential decay.

**Chart 1. Poly(*p*-phenylene) with Aromatic Sulfonate Side Groups (PPPS)**

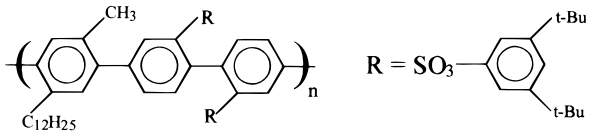


**Table 1. Molecular Characteristics of PPPS Samples[a]**

| sample | $M_n$ (g/mol) | $L_n$ (nm) | $L_w/L_n$ | $L_e$ (nm) | $c^*$ (mg/mL) | $c^{**}$ (mg/mL) |
|---|---|---|---|---|---|---|
| S1 | 99900 | 133.8 | 1.91 | 73.8 | 0.4 | 17.8 |
| S3 | 55400 | 73 | 2.09 | 49.7 | 0.73 | 21.4 |
| S7 | 22000 | 29.7 | 1.82 | 24.8 | 2.39 | 34.9 |
| S9 | 16500 | 22.3 | 1.64 | 19.4 | 3.74 | 42.7 |
| S10 | 8150 | 11 | 1.42 | 10.2 | 12.6 | 75.8 |

[a] Overlap concentrations, $c^*$, and $c^{**}$ correspond to toluene solutions.

## III. Experimental Section

**Materials.** The synthesis of hairy-rod poly(*p*-phenylenes) with aromatic sulfonated side groups, abbreviated as PPPSs with the detailed structure of the side chains depicted in Chart 1, has been reported elsewhere.[10] In the present work a series of PPPSs with different molecular weights was utilized. The molecular characteristics are summarized in Table 1 (the overlap concentrations for semidilute and concentrated regions are c* and c**, respectively; $L_w$ is the weight average contour length, $M_n$ the number average molecular weight, and $L_w/L_n$ the polydispersity). For the present wormlike chains the overlap number concentration $\rho^*$ was approximated by $\rho^* = 1/L_e{}^3$, and $\rho^{**}$ by $\rho^{**} = 1/bL_e{}^2$ as in the case of studies on other PPPs.[9] These specific molecules were chosen because of their large inherent optical anisotropy and the enhanced solubility in common organic solvents, allowing thus the study of the orientational dynamics well into the concentrated region. Solutions were prepared by dissolving the appropriate amount of PPPS in spectroscopic grade solvent (toluene, chloroform, and trichloroethylene, TCE) under continuous stirring for several hours at concentrations below 4 mg/cm$^3$. Dust-free solutions were subsequently obtained by careful filtration of the dilute solutions through a 0.22 $\mu$m Teflon Millipore filter into a dust-free light scattering cell (diameter 10 mm). Higher concentrations were obtained by slow evaporation of the solvent.

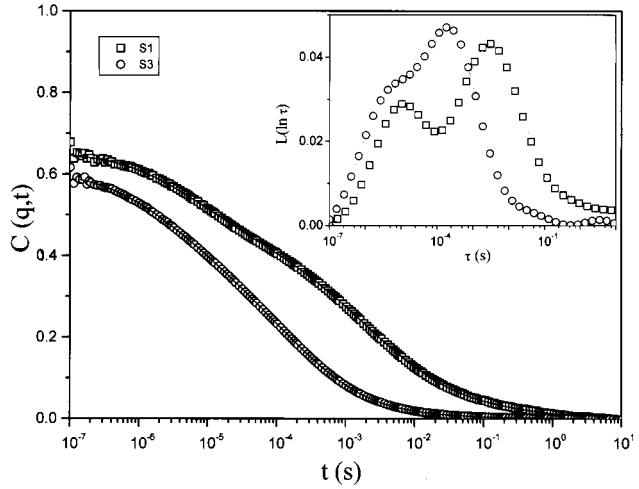


**Figure 1.** Experimental orientational relaxation functions at $q \approx 9 \times 10^{-3}$ nm$^{-1}$ for PPPS S1 (□, 65.6 wt %) and S3 (○, 17.5 wt %) in toluene and chloroform, respectively. The two distributions $L(\ln \tau)$ of relaxation times (eq 9) which represent well (solid lines) the experimental $C(q,t)$ are shown in the inset.

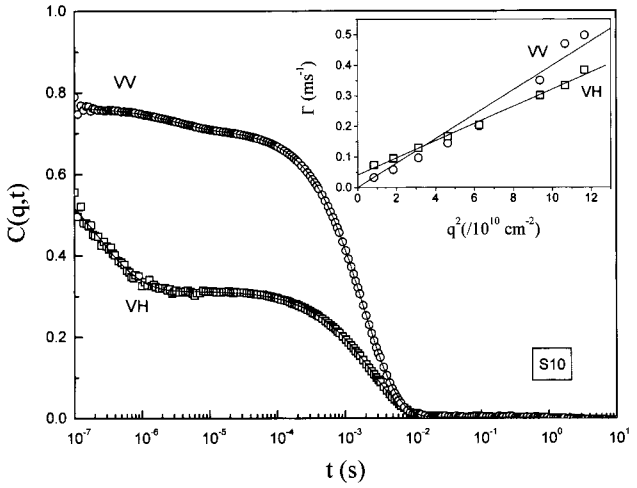


**Figure 2.** Experimental concentration and orientation correlation functions measured, respectively, with dynamic polarized (VV, ○) and depolarized (VH, □) light scattering from 20% solution of PPPS S10 in toluene at $q = 3.4 \times 10^{-2}$ nm$^{-1}$ and 25 °C. The inset shows the variation of the respective slow relaxations with $q$.

**Photon Correlation Spectroscopy (PCS).** The autocorrelation function $G(q,t) = \langle I(q,t)\, I(q,0)\rangle / \langle I(q,0)\rangle^2$ of the depolarized (VH) light scattering intensity, $I(q)$, at a scattering wavevector $q = (4\pi n/\lambda)\sin(\theta/2)$ ($n$ is the refractive index of the medium, $\lambda$ the wavelength of the incident beam, and $\theta$ the scattering angle), was measured with an automated ALV goniometer and an ALV-5000 full digital correlator (320 channels) over the time range $10^{-7}-10^{3}$ s. The light source, polarized vertically (V) to the scattering plane, was a Nd:YAG dye-pumped, air-cooled laser (Adlas DPY 325) with a single mode intensity of 100 mW and $\lambda = 532$ nm. The scattered light was polarized horizontally (H) with respect to the scattering plane by means of a Glan-Thompson analyzer with an extinction ratio better than $10^{-7}$. The measured homodyne normalized light scattering intensity autocorrelation function $G(q,t)$ is given by the Siegert relation[7,19]

$$G(q,t) = 1 + f^* |\alpha g(q,t)|^2 \tag{8}$$

where $f^*$ is an experimental instrument factor (which relates the scattering area with the coherence area) calculated by means of a standard, α is the fraction of the total scattered intensity arising from fluctuations with correlation times longer than $10^{-7}$ s, and $g(q,t) = \langle E^*(q,0)E(q,t)\rangle / \langle |E(q0)|^2\rangle$ is the normalized field correlation function, where $E(q,t)$ stands for the scattered electric field. During the accumulation time, the average light scattering intensity remained constant. Two procedures were chosen for the analysis of the experimental correlation functions, $C(q,t) \equiv \alpha g(q,t)$:

(i) Inverse Laplace transformation (ILT), using the program CONTIN.[22] This method assumes that $C(q,t)$ can be represented by a superposition of exponentials

$$C(q,t) = \int L(\ln \tau) \exp(-t/\tau) d(\ln \tau) \tag{9}$$

which determines a continuous spectrum of relaxation times $L(\ln \tau)$; the characteristic relaxation times, $\tau$, correspond to the maximum values of $L(\ln \tau)$. Typical VH experimental autocorrelation functions $C(q,t)$ over 8 decades in time at $\theta = 30°$, are shown in Figure 1 for S1 ($c = 65.6\%$, $c/c^* = 1396$, in toluene) and S3 ($c = 17.5\%$, $c/c^* = 208$, in chloroform) in the concentrated regime.

(ii) In the case of a single relaxation process, the nonexponentiality of $C(q,t)$ can be described by the Kohlrausch−Williams−Watts (KWW) function[6,19]

$$C(q,t) = A \exp[-(t/\tau)^{\beta}] \tag{10}$$

where $\beta$ is the shape parameter ($\beta = 1$ corresponds to a single-exponential process).

**Shear Rheology.** The dynamic storage ($G'$) and loss ($G''$) moduli of solutions of S1 and S7 at various concentrations, ranging from the dilute to the concentrated regimes, were measured using small-amplitude oscillatory shear experiments. A Rheometric Scientific constant strain rheometer (model ARES-HR with a very sensitive dual-range force rebalance transducer 100FRTN$_1$ and a high-resolution actuator) was utilized. Measurements were carried out in the cone-and-plate geometry (25 mm diameter, 0.04 rad cone angle) at room temperature, and in an atmosphere saturated in solvent (toluene) to eliminate solvent evaporation during measurements. Dynamic strain sweep (at constant frequency, from 1 to 100% strain amplitude) and frequency sweep (at constant strain, from 500 to 0.05 rad/s frequency) tests were performed to determine the regime of linear viscoelasticity and obtain the frequency-dependent shear moduli, i.e., the storage, G′, and loss, G″, moduli.

## IV. Results and Discussion

**A. Overall Picture: The Origin of Orientation Relaxation.** Figure 1 shows the experimental time orientational correlation function $C(q,t)$ for two PPPS solutions in two different solvents at 25 °C and scattering angle 30°. A two-step relaxation is clearly evident from the $C(q,t)$ of S1, as well as the distribution relaxation functions $L(\ln \tau)$ (eq 9) of the two solutions irrespective of $M_w$ and solvent (toluene, chloroform and TCE). For all samples but S10 above about 6%, in three different solvents, $C(q,t)$ conforms to this bimodal relaxation and is distinctly different from the isotropic light scattering (from concentration fluctuations) over the same time range.[11] These two pertinent findings strongly support the molecular origin of this bimodal orientation relaxation, observed also in chemically dissimilar PPPs.[9b]

Alternatively, nonmolecular factors, such as aggregation, would lead to unique isotropic and anisotropic scattering[9b,23] displayed by the low molecular weight S10 solutions in toluene in Figure 2. The slow process in the concentration and orientation relaxation functions assumes similar dynamics with $q$-dependent rates characteristic of optically anisotropic clusters with translational and rotational diffusion. Like in all other

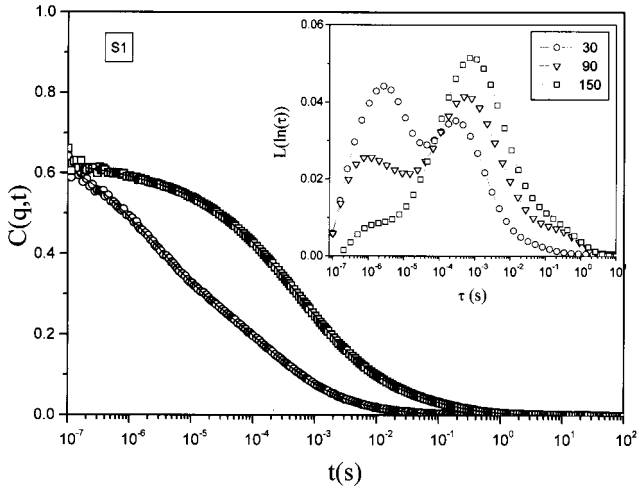


**Figure 3.** Experimental orientational relaxation functions for 38.6% S1 in toluene at two wave vectors (○, $9 \times 10^{-3}$ nm$^{-1}$; □, $3.4 \times 10^{-2}$ nm$^{-1}$) and 25 °C. The distribution of orientation relaxation times for three scattering wave vectors (angles 30°, ○; 90°, ▽; and 150°, □) is shown in the inset.

samples (Figure 1), the fast process of $C(q,t)$ in Figure 2 relates to the molecular orientation dynamics.[7,9] An additional support of the molecular origin of the relaxation functions in Figure 1 is provided by the presence of enhanced short-range orientation fluctuations in these PPPS solutions. As shown in Figure 3 for a 38.6% (by weight) S1 solution in toluene, the contribution of the peak at long times in $L(\ln \tau)$ (cf. Figure 1) increases with $q$; aggregation would lead to stronger forward (low $q$ values) light scattering.[9b]

Figure 3 reveals spatial correlations in the orientation fluctuations associated with the second (slow) process of the $C(q,t)$ providing evidence of the presence of local ordering[9b] (see also section IV.B). The unusual bimodal shape of $C(q,t)$, which does not relate to aggregation phenomena, has been neither predicted theoretically for either rigid or semiflexible polymers (section II.A) nor adequately characterized experimentally, owing to limited solubility.[9] To establish the phenomenology of this unusual orientation relaxation behavior, the variation of $C(q,t)$ with the wavelength ($q^{-1}$) of the fluctuations and solute concentration was thoroughly examined for five PPPS samples. The relaxation rates and intensities were obtained respectively from the position and integration of the peaks in $L(\ln \tau)$ (Figures 1 and 3). The variation of the rate $\Gamma_f$ and the intensity $I_f$ associated with the fast process, with $q$, suggests spatial correlation in the random orientation fluctuations of the isotropic solutions; the coherence length, $\xi$, of the orientational fluctuation correlations is $O$ (40 nm) (see also section IV.B). In contrast, the $q$-dependence of the contribution of the new slow process is unusual (section IV.C). It was found to increase with $q$ for all PPPS samples, as demonstrated in Figure 4 for three solutions of S1 in toluene at 25 °C. The variation of $I_s$, associated to the slow process, with $q$, suggests nonrandom orientation correlations over some characteristic distance. These main findings for the bimodal $C(q,t)$ will be discussed in the next section.

From the phenomenological evidence above, and in view of the lack of theoretical approaches addressing this problem, and in particular the unusual $q$-dependence of the slow mode, we develop the following tentative qualitative picture of the collective orientation dynamics of hairy-rod polymers: The fast process is assigned to the collective random rotational motion of segments of the PPPS chains, typically of the size of the persistence length. On the other hand, in addition to their collective rotational relaxation leading to randomly correlated in space orientational fluctuations, pairs of such Kuhn segments can exhibit orientational correlations, which can be considered as a kind of local ordering; the latter would give rise to a peak in the scattering intensity at finite $q$ values. This situation, which essentially represents two "dynamic populations", namely, orientationally correlated single Kuhn segments and pairs of Kuhn segments, is schematically illustrated in Figure 5. The figure attempts to depict a snapshot of a concentrated solution of a hairy-rod polymer. The Kuhn segments are relaxing their orientation correlations through a "classical" rotational diffusion-like mechanism (section II.B). The space correlation between orientations of neighboring Kuhn segments can persist over a typical coherence length that defines the size $\xi$ of (hypothetical) swarms.[24] The latter can be visualized as orientationally correlated regions, randomly correlated in space, with local orientational ordering.

This tentative picture of the spatial-orientational order of the hairy-rod polymers, which supports qualitatively the main experimental findings, will be justified in detail in the following sections.

**B. Bimodal Orientation Relaxation Function.** The insensitivity of the orientation dynamics to the choice of three nominally good solvents was thoroughly examined for S3 in toluene, $CHCl_3$, and TCE for solute concentrations up to 20%; in $CHCl_3$, higher concentrations led to opaque solutions. As mentioned in the preceding section, the bimodal shape of $C(q,t)$, resolved above about 6% (by weight), is present in all three solvents. The average depolarized intensity, $I$, associated with the two processes of Figure 1 for $c > 6\%$ and the solute contribution (accounting for the solvent intensity) for $c < 6\%$, where their dynamic resolution was ambiguous, are compared among the solutions in the three solvents in Figure 6. The same figure includes the relaxation rates of the two processes in the limit $q \rightarrow 0$ at different S3 concentrations in the three solvents. The observed good agreement, within experimental error, for both static and dynamic data clearly supports unchanged chain conformation and interactions in the three solvents; up to about 20% the total $I$ increases linearly with the concentration of the anisotropic molecular scatterers. Note that these solvents do not possess the same quality as judged from the intensity of a slow process in the isotropic light scattering.[11]

The unusual bimodal shape of $C(q,t)$, which does not relate to aggregation, is an intrinsic property of the present hairy-rod-like polymers. The slow process exhibits a distribution of relaxation times as indicated by the broad (more than 2 decades in time) width of $L(\ln \tau)$; a representation of the second process of $C(q,t)$ by eq 10 yields values of $\beta$ between 0.3 and 0.4 for the high q values of Figure 3 at which the slow relaxation dominates. For comparison the fast process of $C(q,t)$ appears to display narrower distribution as reflected in the higher $\beta$ ($=0.65 \pm 0.05$) obtained from the representation of the experimental $C(q,t)$ at low $q$ values by a double KWW equation. In view of eq 2, the polydisperse nature (distribution of chain lengths) of the samples (Table 1) might account for the nonexponential shape of the fast process. The most probable relaxation

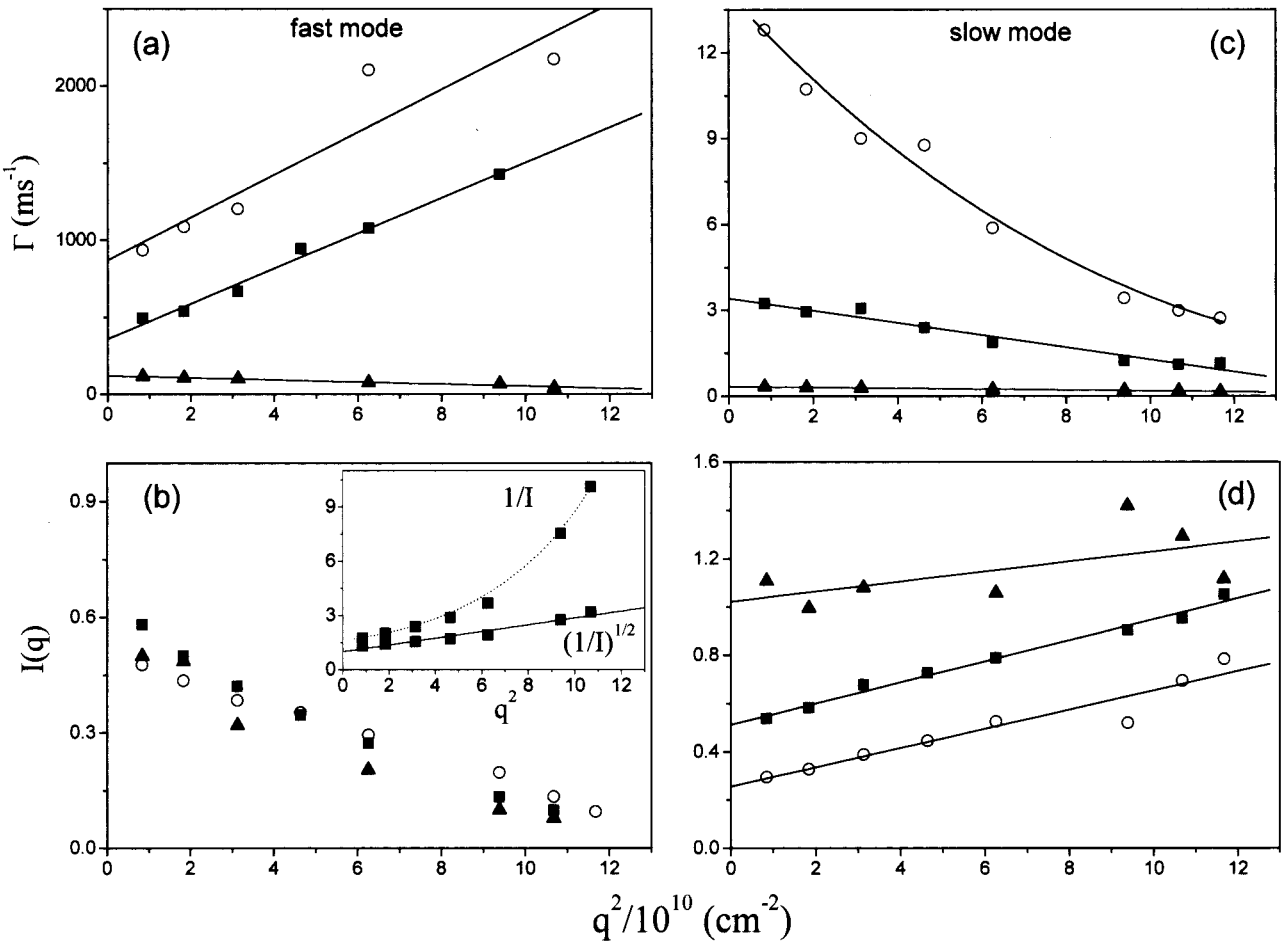


**Figure 4.** Depolarized rate Γ (a, c) and intensity, normalized to the polarized intensity of toluene, $I(q)$ (b, d) of the two processes of $C(q,t)$ for three concentrations of S1 solution in toluene (22.6, ▲; 38.6, ■; 65.6 wt %, ○) as a function of the square of the scattering wave vector, $q^2$. The solid lines represent the best fits. Inset: Debye-Bueche ($I^{-1/2}$) and Ornstein−Zernicke ($I^{-1}$) representations of the orientational correlation fluctuations of the fast process ($I_f$) for the 38.6% solution of S1 in toluene. Solid and dashed lines represent the respective fits.

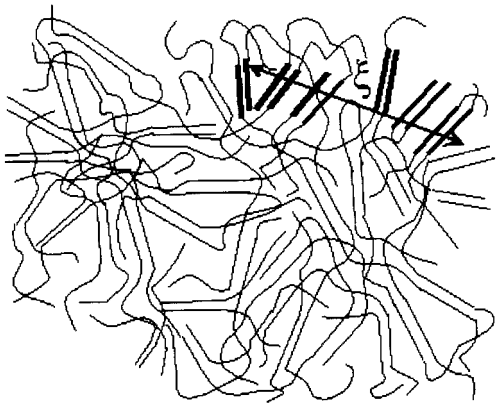


**Figure 5.** Schematic representation of the local orientational order and correlations over a distance $\xi$ (see text) in entangled semistiff chains. Few pairs of locally oriented Kuhn segments are shown with bold lines.

rates (at the peak maxima of $L(\ln \tau)$) and the intensities of the two processes display reciprocal relationships to $q$. The contribution of the main (slow) mode with broad distribution of relaxation times increases while it becomes slower, and its intensity increases with increasing q for all PPPS samples as demonstrated in Figure 4 for three concentrations of S1 in toluene at 25 °C. For the slow process (Figure 3) of $C(q,t)$, short range (and hence high $q$) orientation fluctuations are more probable and decay slower than long wavelength fluctuations, as indicated by the variation of $I_s(q)$ and $\Gamma_s(q)$ with $q$. This interplay is reminiscent of the effect of interactions on collective dynamics, exclusively so far observed for composition fluctuations in systems exhibiting an ordering transition with mesoscopic length scales.[25]

On the other hand, the fast $\Gamma_f$ (Figure 4) is found to increase moderately with $q$ as expected for optically anisotropic scatterers undergoing rotational and translational diffusion (eq 5). The intensity $I_f$ associated with this process should either be virtually $q$-independent for $q\xi < 1$ or decrease with $q$ for larger size. The latter is unlikely if the characteristic size is the persistence length ($l \sim 25$ nm).[6,11] An alternative possibility would be the increase of the coherence length $\xi$ of orientational fluctuation correlations in the isotropic region approaching the nematic phase transition in molecular liquid crystals[24,27] (see section IV.C below). The observed decrease of $I_f$ with $q$ for all samples was found to compensate roughly the corresponding increase of $I_s$ as indicated by the insensitivity of the total $I$ ($=I_f + I_s$) to $q$ variations. In the same context, the intensity $I$ was found to scale linearly with $c$ (Figures 6 and 7 below), which implies overall negligible orientation correlations. The static $I$ alone could therefore lead to misinterpretation of its $q$- and $c$-dependence without the ability to measure the dynamics of the orientation fluctuations.

The concentration dependence of $I$ and its contributions, $I_f$ and $I_s$, which is a sensitive index of static

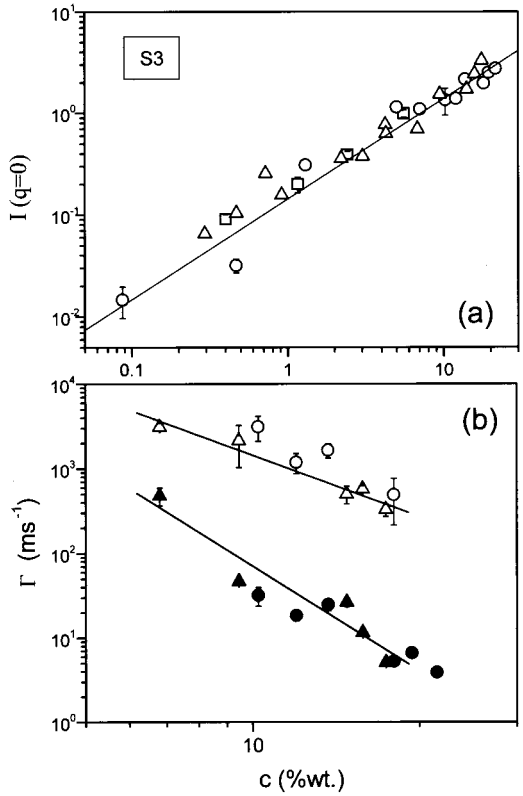


**Figure 6.** Depolarized light scattering intensity (a), normalized to the polarized intensity of toluene, and rate (b) of the two processes (fast: open symbols; slow: closed symbols) of $C(q,t)$ in the thermodynamic limit $q \rightarrow 0$ for PPPS S3 solutions in three solvents: TCE (○), $CHCl_3$ (△), and toluene (□). Above about 6% dynamic resolution is feasible and $I(q = 0)$ refers to the intensity of the two processes.

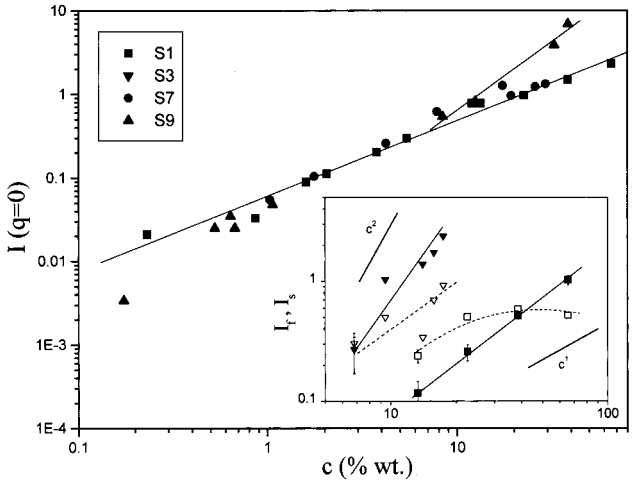


**Figure 7.** Concentration dependence of the total depolarized $I$ and its contributions $I_f$ (closed symbols) and $I_s$ (open symbols), shown separately in the inset, for various PPPS solutions (■, S1; ▼, S3; ●, S7; ▲, S9). All intensities refer to the thermodynamic limit. Lines are drawn to guide the eye. As indicated in the inset, $I_f$ seems to scale with $c^2$ whereas $I_s$ seems to scale with $c^1$.

orientation correlations (eq 3), is visualized for all samples in Figure 7 and its inset, respectively. Pertinent information is included in this figure. Below about 6%, all samples but S3 (cf. Figure 6) display experimentally the same $I$ indicating the semiflexible nature of PPPS already above S9, i.e., the optical molecular anisotropy[6] $\langle\gamma^2\rangle \propto L$. The virtually linear increase of $I$ with concentration implies isotropic solution of orientationally uncorrelated Kuhn segments of size $l$. For $c > 6\%$, the dynamics of orientation fluctuations fall into the PCS time window and the resolution of the two processes (Figures 1 and 3) allows the estimation of $I_f$ and $I_s$ (inset of Figure 7). The linear relationship $I \propto c$ persists up to the highest $c$ for S1, S3, and S7 with the exception of the less flexible S9 ($L \sim l$) for which $I$ increases stronger than $c$. The two intensity contributions show different $c$-dependence with $I_s$ varying stronger than $I_f$, due probably to enhanced orientational pair interactions (section IV.D). The latter should also affect the variation of the collective rate $\Gamma_s$ with $c$ as opposed to $\Gamma_f(c)$, which is examined next.

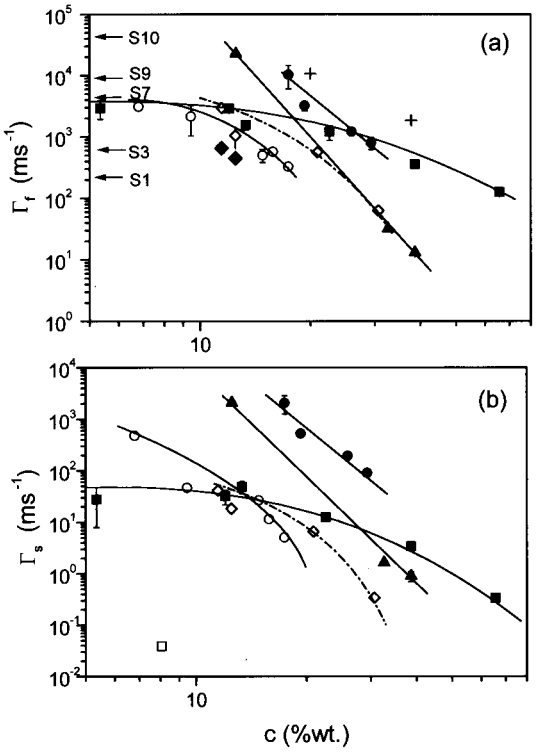


**Figure 8.** Concentration dependence of the two relaxation rates $\Gamma_f$ (a) and $\Gamma_s$ (b) obtained from the inversion of the orientation correlation functions (■, S1; ○, S3; ●, S7; ▲, S9; +, S10; ◇, S1/S9 mixture, first mode; ◆, S1/S9 mixture, second mode). Lines are drawn to guide the eye. The horizontal arrows indicate estimates of the rotational diffusion rate, $6D_{R,0}$ for the various semistiff chains. The longest relaxation time (overall chain rotation) from rheology (Figure 9) is also shown for S1 (□) in (b).

Since both $\Gamma_f$ and $\Gamma_s$ depend on $q$ (Figure 4), Figure 8 depicts the $c$-dependence of these quantities at $q \rightarrow 0$. At a first glance, the separation of the two relaxation rates increases with $c$ reflecting the stronger $c$-dependence of $\Gamma_s$. The variation with concentration is stronger than $c^{-2}$ (eq 2) for both rates, which much like the bimodality of $C(q,t)$ does not conform to the mean-field theoretical predictions for rigid-rod or semistiff polymers (section II.A). In the same context, an estimation of the rotational diffusion rate, $6D_R$, in the dilute regime for semistiff rods,[28] leads to systematically smaller values (arrows in Figure 8) than anticipated from the experimental $\Gamma_f$ rates, which suggests slower dynamics of the overall rotation of the chain.

We complement the dynamic depolarized light scattering data with information on the dynamic shear moduli for two PPPS samples at different concentrations. As seen in Figure 9, the linear viscoelastic data ($G'$, $G''$, and the complex viscosity $\eta^*$) of a concentrated

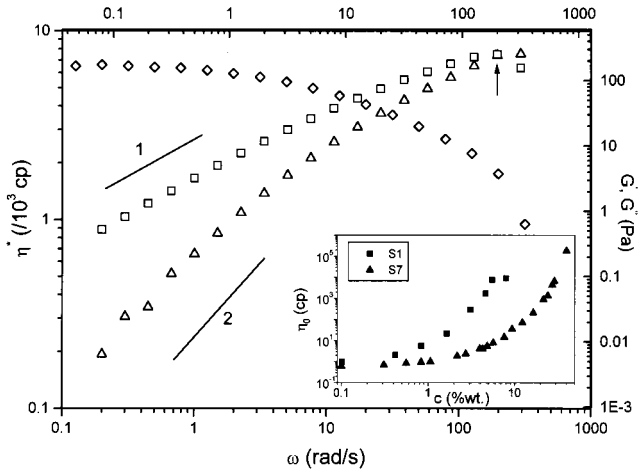


**Figure 9.** Frequency dependence of the dynamic shear moduli (storage, $G'$, △; loss, $G''$, □) for a typical semidilute S1 solution in toluene (8%) at 25 °C. The $G' - G''$ crossover identifies the longest relaxation time (vertical arrow). The complex dynamic shear viscosity, yielding the solution's zero-shear viscosity, $\eta_0$, is also shown in the plot (◇). Slopes indicate terminal regime scaling. Inset: Concentration dependence of $\eta$ for S1 (■) and S7 (▲) in toluene.

entangled 8% (by weight) S1 solution in toluene, at 25 °C, exhibit the standard terminal regime scaling behavior ($G' \sim \omega^2$ and $G'' \sim \omega$), which allows the straightforward estimation of the longest chain relaxation time $\tau$ and the zero-shear viscosity $\eta_0$ ($=G''/\omega$, at low frequencies).[29] The measured solution viscosities also exhibit a much stronger than $c^2$ dependence (inset of Figure 9), in qualitative agreement with the sharp concentration dependence of both $\Gamma_f$ and $\Gamma_s$. From Figures 8 and 9 it is clear that the measured longest viscoelastic relaxation rates are much slower (by nearly 2 decades) than the slowest orientational relaxation rates. This can be explained by the fact that the longest viscoelastic relaxation in the present experiments is actually the disentanglement time (chain orientation relaxation time) in the transient physical networks formed at the high concentrations investigated, whereas on the other hand the detected rates $\Gamma_f$ relate to orientations of Kuhn segments, i.e., length scales shorter than the chain length.

Aside from the disagreement with the theory of rigid rodlike polymers, the slowing down of $\Gamma_f$ and $\Gamma_s$ with concentration becomes systematically stronger with decreasing $L/l$. Hence at high concentrations, orientation fluctuations relax faster in S1 than in S9 despite the fact that S1 is about six times more concentrated (the ratio of $c^*$ values for S9 and S1). Since the PPPS samples possess the same static flexibility ($l =$ constant) (Figure 7), this unexpected result might reflect the cooperative nature of the dynamics of the contour fluctuations in agreement with the broad $L(\ln \tau)$ distribution of the slow process. To verify this conjecture, we examine how the orientation dynamics of an equimolar S1/S9 mixture in toluene above 10% compare to the relaxation function of the individual components.

Despite the fact that the two components have quite different orientational dynamics at low (∼10%) and high (∼30%) concentrations (Figure 8), two processes still contribute to the experimental $C(q,t)$ of the equimolar S1/S9 solution in toluene, and the two rates are shown in Figure 8. In a miscible system, this relaxational behavior provides strong evidence of dynamic cooperativity which is, moreover, supported by the domination of the slow component in the mixed ternary solution; $\Gamma_f$ and $\Gamma_s$ are close to the corresponding rates of S1 and S9, respectively, at about 10% and 30%; i.e., the slow component determines the mixture orientational dynamics. The depolarized intensities $I$, $I_f$, and $I_s$ show no measurable changes in the S1/S9 solution and are expectedly similar to these in S1 with the higher weight concentration. It appears therefore that the strong $c$-dependence of $\Gamma_f$ and $\Gamma_s$ results from the increased cooperativity with c that is reminiscent to the glass dynamics. The good solubility and the absence of mesophases in the PPPS enable the investigation of the isotropic phase in the concentrated regime. The lack of a transition to a nematic phase, in contrast to what is expected from the stiff character of the polymer chain, might be due the existence of the side chains, which preclude a long range parallel packing of the molecules.

**C. Fast Orientation Fluctuations: Kuhn Segment Rotation.** On the basis of the $q$-dependence (Figure 4) of $\Gamma_f$ and its relationship to $\eta_0$, the fast decay in $C(q,t)$ can be assigned to the collective rotational motion of the Kuhn segments of the persistent PPPS chains. In the concentrated regime, this motion is strongly restricted as reflected in the strong $c$-dependence of $\Gamma_f$ (Figure 8). The time average correlation between the orientations of neighboring Kuhn segments can persist over a certain distance, i.e., the coherence length $\xi$ defining the size of orientationally correlated regions (the swarms illustrated in Figure 5).[24] The orientational ordering in the isotropic phase is usually local and $I_f$ is virtually $q$-independent since $q\xi \ll 1$. For the present systems, however, Figure 4 reveals a $q$-dependence for $I_f$ at high concentrations, which cannot adequately be represented by the Ornstein−Zernicke type of orientation correlations[19] ($f(r) = \exp(r/\xi)/r$), predicting $I(q)^{-1} \propto 1 + q^2\xi^2$ (inset of Figure 4). Instead, $I(q)^{-1/2} \propto 1 + q^2\xi^2$, which implies Debye−Bueche orientation correlation function[30] ($f(r) = \exp(r/\xi)$), provides a better description of the experimental $I_f$.

Among the samples, S1 and S3 with the largest length $L/l$ values, as well as the equimolar S1/S9 ternary solution, display the strongest $q$-dependence for $I_f$, which moreover increases with concentration; for S1, $\xi$ varies between 30 and 45 nm over the concentration range 11.6−66%, whereas for S3, $\xi = 35$ nm at $c = 17.5\%$. For S7 and S9, the rate of decrease of $I_f$ with $q$ is significantly weaker and rather insensitive to concentration variations over the range 15−40%. It appears, therefore, that the dynamically more flexible S1 and S3 chains ($\Gamma_f$ in Figure 8a) exhibit orientational fluctuation correlations on the average over a longer distance ($\xi = O(50$ nm)) than the shorter S7 and S9 with local scale ($\xi < 20$ nm). The orientation fluctuations associated with the fast mode are randomly correlated (in all directions) in space, and hence the orientation correlated regions are on the average spherical in space leading to a maximum $I_f$ in the forward ($q \to 0$) direction.

The collective orientation fluctuations in dense semiflexible polymer systems (eqs 3 and 6) appear to decay mainly via rotational motions of the Kuhn segments (this situation is schematically illustrated in Figure 5) and should therefore be insensitive to $L$ variations. The much slower overall rotational motion of the chain, with a rate $D_R(c)$ (section II.A), does not appreciably modify the orientational part of $C(q,t)$ (preexponential part of eq 3), and hence the decay of $C(q,t)$ is an insensitive probe of $D_R$. In fact, the viscoelastic longest relaxation

time (e.g., Figure 9) $\tau = D_R^{-1}$ is much slower than $\tau_f$ (as well as $\tau_s$), as already discussed (see also Figure 8b).

**D. Slow Orientation Fluctuations.** The unusual increase of $I_s$ with $q$ indicates another sort of orientation correlation in the nanometer length scales in concentrated isotropic semistiff polymer solutions. A 4-fold clover leaf depolarized light scattering pattern with an off-axis intensity peaks has been reported for crystalline polymers[31] and more recently in nematic liquid crystalline polymers and microphase separated diblock copolymers.[32] Suppression of the forward scattering with a peak of the depolarized intensity at finite $q_{max}$ is possible if the optic axis is allowed to vary within two correlated regions, i.e., for nonrandom orientation correlations.[33] The average domain size, e.g., spherulites,[31] distances between disclination lines[32a] and ordered grains[32b] relates to $q_{max}$ and for these systems is of the order of micrometers, i.e., the intensity peaks at very low scattering angle $\theta_{max}$ (0.5−2°).

For the present isotropic PPPS solutions, $I_s$ (Figure 4) attains no maximum value up to the highest light scattering $q$ ($\approx$0.034 nm$^{-1}$) indicative of the involvement of short sizes, $O$ (nm). Such orientational ordering was inferred from small angle neutron scattering measurements of the structure factor of isotropic solutions of rigid poly($\gamma$-benzyl L-glutamate).[34] If we associate $I_s$ with orientationally correlated Kuhn-segment-pairs, the intersegmental distance should determine $q_{max} \approx 2\pi(c/M)^{1/3}$. In this oversimplified picture (see Figure 5), the increase of $I_s$ with $q$ should be more pronounced in S1 than in S9 at similar concentrations and less evident at high $c$, as for both cases $q_{max}$ shifts to higher values. In fact, these trends are supported by the experimental $I_f(q)$ of the PPPS solutions (Figure 4).

The reciprocal $q$-dependencies of $I_f$ and $I_s$ (Figure 4) indicate, according to the preceding discussion, the presence of preferred local orientational ordering (size $\sim q_{max}^{-1}$). The much slower rate $\Gamma_s$ reflects the cooperative motion of the correlated Kuhn segment pairs. In this structural picture, the unexpected and unusual slowing down of $\Gamma_s$ with $q$ corroborates the notion that the most probable short wavelength fluctuations are long-lived. In principle, this effect of interactions is foreseen by eq 7, since the collective rate $\Gamma(q) \sim \Phi(q)$. It appears that the decrease of $\Gamma_s(q)$ with $q$ (Figure 4) is roughly compensated by the increase of $I_s(q)$ ($\propto\Phi(q)^{-1}$). The slower rate $\Gamma_s$, as compared to $\Gamma_f$, is rationalized by the larger size of the correlated Kuhn segment pairs, whereas its steeper $c$-dependence (Figure 8) resembles the disparity in the variation of the associated intensities $I_s$ and $I_f$ (inset of Figure 7) with concentration. This relationship is dictated by the collective nature of both processes and is more pronounced for the shortest S9.

## V. Conclusions

The dynamics of orientation fluctuations in model poly(*p*-phenylenes), PPPS, have been investigated using dynamic depolarized light scattering. The broad dynamic range of this technique (photon correlation spectroscopy) coupled with the strong inherent optical anisotropy and enhanced solubility of PPPS, provide unique and powerful information on the collective orientation dynamics of hairy-rod polymers. The measured high-quality orientation relaxation functions revealed a bimodal decay of the orientation fluctuations. The fast process was characterized by an intensity decreasing with the scattering wavevector q following a Debye-like behavior and a rotational rate, $\Gamma_f$, with an intercept. On the other hand, the broad slow process had an intensity increasing and a rate, $\Gamma_s$, decreasing with $q$. The concentration dependence of these relaxation modes in different solvents supported the notion of unchanged chain conformation and interactions and revealed a slowing down, which was more pronounced for the slow relaxation. With the additional support of dynamic shear rheological measurements, we have attributed the fast process to the collective rotational motion of the Kuhn segments of the persistent poly(*p*-phenylene) chains and the slow one to the cooperative motion of orientationally correlated pairs of segments. These pertinent findings cannot be explained in the framework of the existing theories for the dynamics of rodlike or wormlike chains and thus represent an important challenge for the understanding of the physics of wormlike hairy-rod polymers in the isotropic regime.

**Acknowledgment.** This research was partially supported by the Greek General Secretariat for Research and Technology (Basic Research Program, PENED-40).

## References and Notes

(1) Tracy, M. A.; Pecora, R. *Annu. Rev. Phys. Chem.* **1992**, *43*, 525. Zero, K.; Pecora, R. In *Dynamic Light Scattering. Applications of Photon Correlation Spectroscopy*; Pecora, R., Ed.; Plenum Press: New York, 1985.
(2) Russo, P. S. In *Dynamic Light Scattering. The Method and Some Applications*; Brown, W., Ed.; Clarendon Press: Oxford, U.K., 1993.
(3) Sato, T.; Teramoto, A. *Adv. Polym. Sci.* **1996**, *126*, 85.
(4) Zero, K.; Pecora, R. *Macromolecules* **1982**, *15*, 87. DeLong, L. M.; Russo, P. S. *Macromolecules* **1991**, *24*, 6139.
(5) McCarthy, T. F.; Witteler, H.; Pakula, T.; Wegner, G. *Macromolecules* **1995**, *54*, 337. Galda, P.; Rehahn, M. *Synthesis* **1996**, 614. Rehahn, M.; Schluter, A. D.; Wegner, G. *Macromol. Chem.* **1990**, *191*, 1991. Kallitsis, J. K.; Rehahn, M.; Wegner, G. *Macromol. Chem.* **1992**, *193*, 1021.
(6) Petekidis, G.; Vlassopoulos, D.; Galda, P.; Rehahn, M.; Ballauff, M. *Macromolecules* **1996**, *29*, 8948. Tiesler, U.; Rehahn, M.; Ballauff, M.; Petekidis, G.; Vlassopoulos, D.; Maret, G.; Kramer, H. *Macromolecules* **1996**, *29*, 6832.
(7) Berne, J. B.; Pecora, R. *Dynamic Light Scattering*; Wiley-Interscience Publications: New York, 1976.
(8) Petekidis, G.; Fytas, G.; Witteler, H. *Colloid Polym. Sci.* **1994**, *272*, 1457.
(9) Petekidis, G.; Vlassopoulos, D.; Fytas, G.; Kountourakis, N.; Kumar, S. *Macromolecules* **1997**, *30*, 919. Petekidis, G.; Vlassopoulos, D.; Fytas, G.; Fleischer, G. *Macromolecules* **1998**, *31*, 1406.
(10) Vanhee, S.; Rulkens, R.; Lehmann, U.; Rosenauer, C.; Schulze, M.; Kohler, W.; Wegner, G. *Macromolecules* **1996**, *29*, 5136.
(11) Petekidis, G.; Vlassopoulos, D.; Fytas, G.; Rulkens, R.; Wegner, G.; Fleischer, G. *Macromolecules* **1998**, *31*, 6139.
(12) Doi, M.; Edwards, S. F. *The Theory of Polymer Dynamics*; Oxford University Press: New York, 1986.
(13) Keep, G. T.; Pecora, R. *Macromolecules* **1985**, *18*, 1167; **1988**, *21*, 817.
(14) Fixman, M. *Phys. Rev. Lett.* **1985**, *54*, 337; **1985**, *55*, 2429.
(15) Sato, T.; Takada, Y.; Teramoto, A. *Macromolecules* **1991**, *24*, 6262.
(16) Odijk, T. *Macromolecules* **1983**, *16*, 1340; **1984**, *17*, 502.
(17) Doi, M. *J. Polym. Sci. Polym. Symp.* **1985**, *73*, 93.
(18) Semenov, A. N. *J. Chem. Soc., Faraday Trans.* **1986**, *82*, 317.
(19) Fytas, G.; Patkowski, A. In *Dynamic Light Scattering. The Method and Some Applications*; Brown, W., Ed.; Clarendon Press: Oxford, U.K., 1993.
(20) Shimada, T.; Doi, M.; Okano, K. *J. Chem. Phys.* **1988**, *88*, 2815.
(21) Maeda. T. *Macromolecules* **1990**, *23*, 1464.
(22) Provencher, S. W. *Macromol. Chem.* **1979**, *180*, 201.

(23) The tendency for aggregation in the low $M_W$ S10 compared to the other samples might be due to the concentration of the chain ends and/or the reduced solubility for low chain flexibility.
(24) de Gennes, P. G.; Prost, J. *The Physics of Liquid Crystals*, 2nd ed.; Clarendon Press: Oxford, 1993.
(25) Boudenne, N. B.; Anastasiadis, S. H.; Fytas, G.; Xenidou, M.; Hadjichristidis, N.; Semenov, A. N.; Fleisher, G. *Phys. Rev. Lett.* **1996**, *77*, 506.
(26) Petekidis, G.; Vlassopoulos, D.; Galda, P.; Rehahn, M.; Ballauff, M. *Macromolecules* **1996**, *29*, 8948. Tiesler, U.; Rehahn, M.; Ballauff, M.; Petekidis, G.; Vlassopoulos, D.; Maret, G.; Kramer, H. *Macromolecules* **1996**, *29*, 6832.
(27) Stinson, T. W.; Lister, J. D. *Phys. Rev. Lett.* **1973**, *30*, 668.
(28) Hearst, J. E.; Stockmayer, W. H. *J. Chem. Phys.* **1962**, *7*, 1425. Hearst, J. E. *J. Chem. Phys.* **1963**, *38*, 1062. Hagerman, P. J.; Zimm, B. H. *Biopolymers* **1981**, *20*, 1481.
(29) Ferry, J. D. *Viscoelastic Properties of Polymers*, 3rd ed.; John Wiley: New York, 1980.
(30) Debye, P.; Bueche, A. M. *J. Appl. Phys.* **1949**, *30*, 518.
(31) Stein, R. S.; Erhardt, P. F.; Clough, S. B.; Adams, G. *J. Appl. Phys.* **1966**, *37*, 3980.
(32) Hashimoto, T.; Nakai, A.; Hasegawa, T.; Rogaczer, S.; Stein, R. S. *Macromolecules* **1989**, *22*, 422. Newstein, M. C.; Garetz, B. A.; Dai, H. J.; Balsara, N. P. *Macromolecules* **1995**, *28*, 4587.
(33) Greco, F. *Macromolecules* **1989**, *22*, 4622.
(34) Wagner, N. J.; Walker, L. M.; Hammouda, B. *Macromolecules* **1995**, *28*, 5075.

MA9804500